Introduction

Many applications in industry and life science have initiated the development of laser sources in the visible spectral range. Important biotechnological, pharmaceutical and medical measurement procedures, such as the confocal microscopy and flow cytometry, are based on laser-induced fluorescence detection technologies. Almost all known human life-threatening diseases can be diagnosed by cytology, the study of the properties of single cells, using tunable visible lasers of a few mW power.
For small hand-held full-color displays red, green, and blue lasers emitting less than 1 mW of total optical power will probably be sufficient. Moreover, three laser beams (blue, green, red) are used for exposing photographic paper, films or printing plates. In addition, depending on the spectral sensitivity of the materials used for these colors, upconversion fiber lasers have the potential to replace one or more lasers in the different setups being used today. Further applications of upconversion fiber lasers are in the field of imaging, metrology, sensing and spectroscopy.
Upconversion fiber lasers offer a good alternative to air-cooled ion lasers and frequency-doubled solid-state lasers. Fiber lasers provide high efficiency, reliable operation, and single-mode beam quality with cost effectiveness. Laser transitions of the Pr^{3+} ion are attractive because laser operation at blue, green, orange and red wavelengths can all be obtained using the same pump source when additionally doping the fiber core with Yb^{3+} ions.
Upconversion lasers may provide a useful route to the development of visible lasers pumped by cheap semiconductor lasers operating in the near infrared region of the spectrum. The emission wavelength of a fiber laser can be adjusted by suitable doping with one or several rare earth ions and additionally be modified by varying the glass composition. The inhomogeneous broadened transitions and thus the broad emission spectra of rare earth ions in glasses enable a spectrally wide tuning range of the emission lines of such lasers by means of wavelength selective resonators.
The discovery of fluoride glass in 1974 originated in a new class of active components in the visible range. This is due to a lower phonon energy which implies a smaller contribution to multi-phonon relaxation, hence, increasing the number of metastable excited levels in fluoride glasses compared to silica hosts. Silica fibers incorporating rare earth ions as the active medium are not particularly adequate for visible lasers. Compared with silica fiber lasers, fluoride fiber lasers offer a wider wavelength range. In practice, most low phonon energy glasses are heavy metals of which ZBLAN glass based on zirconium fluoride is the most famous type, followed by IBZP glass based on indium fluoride.

Spatially resolved determination of the fiber gain of thulium-doped ZBLAN fiber is one main issue of this thesis. In this work, the coherent optical frequency-domain reflectometry (C-OFDR) method is applied to characterize 1050 nm laser diode pumped S-band thulium-doped

fluoride fiber amplifiers (TDFAs). With this measurement technique it is possible to determine the optimum length of the active fiber in amplifier applications without destroying the expensive fluoride fiber. Different thulium concentrations of the active ZBLAN fiber are investigated. Strong cross relaxation processes are expected for highly thulium-doped ZBLAN fibers and will explain the efficient operation of this type of fiber amplifier.
Furthermore, a frequency transfer function (FTF) method is introduced to determine fluorescent lifetimes of arbitrary rare-earth-doped glasses and fibers. The fluorescent lifetime of energy levels of rare-earth-doped glasses or fibers provides a valuable information for fiber laser and amplifier applications. Lifetime measurements for the upper energy levels of praseodymium-doped ZBLAN and IBZP glasses are reported and the influence of ytterbium as co-dopant is shown as well. Concentration quenching is expected for highly praseodymium-doped glass samples. In addition, this work summarizes the fundamental spectroscopic properties of triply ionized praseodymium- and ytterbium-doped ZBLAN glasses.
Special attention is given to the simulation of praseodymium-, ytterbium-, and Pr^{3+}/Yb^{3+}-doped ZBLAN fiber lasers emitting in the visible and infrared spectral range. Simulations allow to reduce the costs of experiments. Experience shows that in the design of a rare-earth-doped ZBLAN fiber laser the suppression of competing laser transitions is as important as the support of desired transitions. Thus, a major part of this work will deal with defining a suitable model which is applicable for arbitrary rare-earth-doped fiber lasers and amplifiers in a variety of configurations. The aim is to find a model which covers steady-state and transient behavior of rare earth devices. Simulations will help to understand the processes, which play a role in the lasing or amplification process and finally, they can be used to find the optimum device parameters and predict the performance of the whole system.

This thesis is organized in six chapters. Their contents is briefly summarized below.

Chapter 1: This chapter summarizes the fundamental processes behind laser operation. Absorption, spontaneous and stimulated emission are described as well as the creation of population inversion.

Chapter 2: In this chapter an overview of exemplary solid-state and semiconductor laser systems is provided. Ruby and fiber lasers are presented as examples of solid-state laser systems, and distributed feedback lasers are presented as an example of semiconductor laser systems.

Chapter 3: The most important properties of rare earth host materials which are important in understanding fiber laser operation are discussed in this chapter. Emphasis is put on basic features of fluoride glasses doped with rare earth ions. An overview of ion interactions and the properties of non-radiative transitions is also given. The latter includes multi-phonon processes and energy transfer mechanisms. The avalanche upconversion pumping scheme of Pr^{3+}/Yb^{3+}-doped lasers is discussed in detail. Finally, the relevant transitions

in praseodymium- and ytterbium-doped fluoride glasses are presented.

Chapter 4: The properties of thulium-doped fluoride fibers used for fiber amplifier applications and of praseodymium-doped fluoride glasses for fiber laser applications are thoroughly discussed in this chapter. The active thulium fiber is spatially characterized by C-OFDR. Moreover, a new frequency transfer function (FTF) method is presented and applied to measure the fluorescent lifetimes of the upper laser levels in praseodymium-doped ZBLAN and IBZP glasses, some of them co-doped with ytterbium.
In the last section of this chapter some important spectroscopic parameters of praseodymium in ZBLAN glass are presented which will be used for fiber laser simulation in chapters 5 and 6. Extensions to the methods developed in this chapter are given in appendix A, B, and C.

Chapter 5: The spectroscopic parameters described in the previous chapter are used in this chapter to simulate different fiber lasers. A stationary model for the simulation of arbitrary rare-earth-doped fiber lasers and amplifiers is presented. The model is applicable for a rare earth ion as dopant in lasers and amplifiers and is applied to the simulation of an ytterbium-doped and to red, orange and blue praseodymium-doped ZBLAN fiber lasers. Maxwell-Boltzmann statistics for thermally coupled energy levels is applied in combination with a novel approach to fix the usually unknown values of non-radiative transition rates for the simulations. Furthermore, the model is extended to simulate cross relaxation processes between two different ions in rare-earth-doped devices. Finally, red, orange and blue characteristics of Pr^{3+}/Yb^{3+}-doped ZBLAN fiber lasers are simulated and compared to the results of Pr^{3+}-doped ZBLAN fiber lasers. The dominance of the avalanche upconversion process in case of the former type of laser is proven by this model.

Chapter 6: In this chapter a novel dynamic model for the simulation of arbitrary rare-earth-doped fiber lasers and amplifiers is presented. A model for a single rare earth ion is presented and extended to model energy transfer processes in lasers and amplifiers doped with two rare earth ions. The model uses the same mathematical concept introduced in chapter 5 and is applied to simulate the transient behavior of ytterbium-doped, praseodymium-doped and Pr^{3+}/Yb^{3+}-doped ZBLAN fiber lasers. Relaxation oscillations of the output power have been observed and these results have been evaluated to extract different parameters of the simulated fiber lasers.

1 Laser theory

In this chapter, the fundamental processes behind laser operation are briefly discussed. In 1917, Albert Einstein showed that the process of stimulated emission must exist, but it was not before 1960 that Maiman was able to demonstrate laser action for the first time [1]. A laser consists of three elements: an active medium, a pump, and a resonator. To make a laser oscillator from an amplifier, it is necessary to introduce suitable positive feedback by means of the resonator. Basic principles and the construction of lasers are relatively simple but, on the other hand, a rigorous analysis of laser physics is quite sophisticated. Thus, the approach described here has been simplified to cover basic laser principles while maintaining a concise theory.

1.1 Interaction of radiation with matter

In order to understand laser operation some of the principles which govern the interaction of radiation and matter have to be known. Atomic systems such as atoms, ions, and molecules can exist only in discrete energy states. A change from one energy state to another is called a transition. To simplify the discussion, let us consider an idealized material with merely two energy levels, 1 and 2, having populations of N_1 and N_2, respectively (see Figure 1.1). The total number of atoms in these two levels N_0 is assumed to be constant:

$$N_0 = N_1 + N_2. \tag{1.1}$$

Let us assume that the system is in the lower level E_1. Then, in the presence of photons, it may be excited to the upper level E_2 by absorbing a photon with energy $E_2 - E_1$. This process is called *absorption*. Alternatively, if the system is in the level E_2, it may return to the ground state with the emission of a photon. The energy difference between the levels must be compensated by the emission of radiative energy and is given by the following relation:

$$\Delta E = E_2 - E_1 = \frac{h \cdot c}{\lambda} = h \cdot \nu_{21}, \tag{1.2}$$

where h is Planck's constant, c the speed of light, ν_{21} the optical frequency, and λ the wavelength of the photon. E_2 and E_1 are energy values corresponding to the two discrete energy levels and ΔE represents their energy difference.
The emission process may occur in two ways: A first possibility is the *spontaneous emission* process in which the system drops to the lower level in a completely random way. The second possibility is the *stimulated emission* process in which the system is 'triggered' by the presence of a photon to make the transition. The photon must have the proper energy corresponding to the energy difference between the original state and the lower energy level. The stimulated

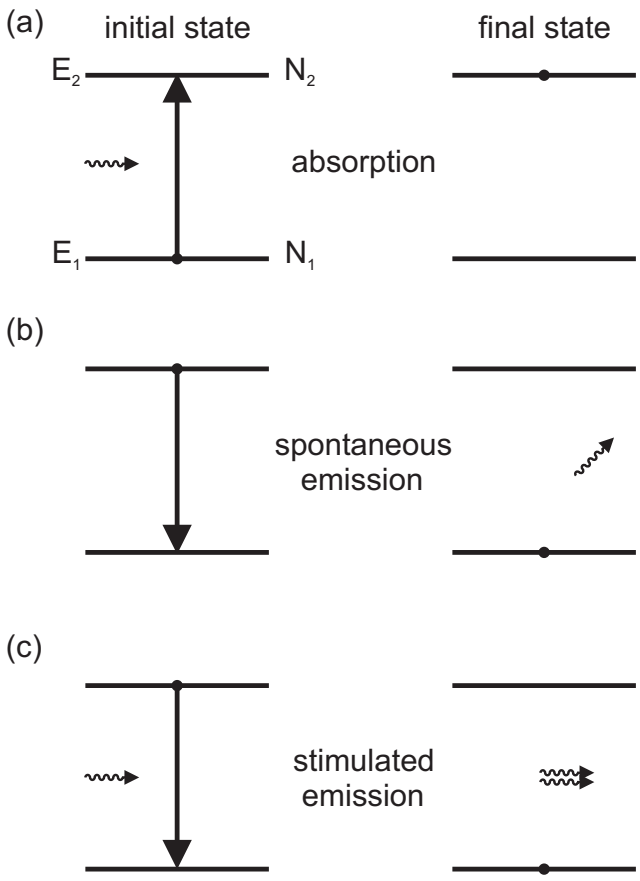

Figure 1.1: Schematic diagram illustrating (a) absorption, (b) spontaneous emission, and (c) stimulated emission

photon has the same frequency, same polarization state, same phase, and it propagates in the same direction as the stimulating photon. This is the fundamental difference between the stimulated and the spontaneous emission processes. In case of the latter one, atoms emit an electromagnetic wave that has no definite phase relation to that emitted by another atom (see Figure 1.1). Furthermore, the wave can be emitted in any direction.
In case of stimulated emission the original radiation is still present, and so the radiation intensity has been amplified. This is the origin of the acronym LASER: *Light Amplification by Stimulated Emission of Radiation*. The three processes are illustrated in Figure 1.1. The horizontal straight lines represent the energy level, the wavy arrows represent photons and the vertical arrows represent the transitions of electrons from one level to another. The black dot indicates the atom state, before (left part of the diagram) and after the transition (right part of the diagram).

1.1.1 Absorption

If a quasi monochromatic electromagnetic wave of frequency ν_{21} passes through an atomic system with energy gap $h \cdot \nu_{21}$, the population of the lower level will be depleted at a rate proportional both to the radiation density $\rho(\nu)$ and to the population N_1 of that level:

$$\frac{\mathrm{d}N_1}{\mathrm{d}t} = -B_{12} \cdot \rho(\nu) \cdot N_1, \tag{1.3}$$

where B_{12} is the coupling constant of radiation and matter for the absorption process (Einstein coefficient). The product $B_{12} \cdot \rho(\nu)$ can be interpreted as the probability per unit frequency that transitions are induced by the electromagnetic field.

1.1.2 Spontaneous emission

After a couple of atoms have been excited to the upper level, the population of the upper level decays spontaneously to the lower level at a rate proportional to the upper level population:

$$\frac{\mathrm{d}N_2}{\mathrm{d}t} = -A_{21} \cdot N_2, \tag{1.4}$$

where A_{21} is the coupling constant for the spontaneous emission process (Einstein coefficient). This coefficient gives the probability for an atom in level 2 to decay spontaneously to the lower level 1 within a unit of time. Spontaneous emission is characterized by the lifetime of the electron in the excited state in which it will spontaneously return to the lower state and radiate the energy difference. This radiative lifetime is related to A_{21} by:

$$\tau_{rad} = \tau_{21} = \frac{1}{A_{21}}. \tag{1.5}$$

In general, the reciprocal transition probability of a process is called its lifetime (see section 4.2).
It is noted that spontaneous radiative emission is merely one of two possible ways for the atom to decay. Decay can also occur in a non-radiative way. In this case the energy difference is delivered in some form of energy other than electromagnetic radiation such as kinetic or internal energy of the surrounding atoms or molecules [2].

1.1.3 Stimulated emission

As has already been mentioned, emission takes place not only spontaneously but also under stimulation. The atom gives a quantum to the radiation field by induced emission:

$$\frac{\mathrm{d}N_2}{\mathrm{d}t} = -B_{21} \cdot \rho(\nu) \cdot N_2, \tag{1.6}$$

where B_{21} is the coupling constant for the stimulated emission process (Einstein coefficient). Combining absorption, spontaneous and stimulated emission, as presented in equations (1.3), (1.4) and (1.6), one can write for the change of the upper and lower level populations in the two-level model:

$$\frac{\mathrm{d}N_1}{\mathrm{d}t} = -\frac{\mathrm{d}N_2}{\mathrm{d}t} = B_{21} \cdot \rho(\nu) \cdot N_2 - B_{12} \cdot \rho(\nu) \cdot N_1 + A_{21} \cdot N_2. \tag{1.7}$$

For a system in thermal equilibrium, the number of transitions per unit time from E_1 to E_2 must be equal to the number of transitions from E_2 to E_1. Hence, one gets:

$$A_{21} \cdot N_2 + B_{21} \cdot \rho(\nu) \cdot N_2 = B_{12} \cdot \rho(\nu) \cdot N_1, \tag{1.8}$$

which means that the sum of the rates for spontaneous and stimulated emission must be equal to the absorption rate in thermal equilibrium. Thus, one obtains for the radiation density

$$\rho(\nu) = \frac{A_{21}/B_{21}}{\frac{B_{12}}{B_{21}}\frac{N_1}{N_2} - 1}. \tag{1.9}$$

The populations of the energy levels 1 and 2 in thermal equilibrium are given by Boltzmann statistics:

$$\frac{N_1}{N_2} = \frac{g_1}{g_2} \exp\left(\frac{\Delta E}{k_B T}\right) = \frac{g_1}{g_2} \exp\left(\frac{h \cdot \nu_{21}}{k_B T}\right), \tag{1.10}$$

where k_B is Boltzmann's constant, T is the absolute temperature of the material in Kelvin and g_j is the degeneracy of level j. Hence, substituting equation (1.10) into (1.9) yields

$$\rho(\nu) = \frac{A_{21}/B_{21}}{\frac{g_1}{g_2}\frac{B_{12}}{B_{21}} \cdot \exp\left(\frac{h \cdot \nu_{21}}{k_B T}\right) - 1}. \tag{1.11}$$

The atom system is considered to be in thermal equilibrium, thus it must give rise to radiation which is identical with blackbody radiation, the density of which was described by Planck:

$$\rho(\nu) = \frac{8\pi h \nu^3}{c_0^3} \frac{1}{\exp\left(\frac{h \cdot \nu}{k_B T}\right) - 1}. \tag{1.12}$$

Comparing equations (1.11) and (1.12), one concludes:

$$\frac{A_{21}}{B_{21}} = \frac{8\pi h \nu^3}{c_0^3} \quad \text{and} \quad B_{21} = \frac{g_1 B_{12}}{g_2}. \tag{1.13}$$

The relation between the A's and B's are known as Einstein's relations, and, as already mentioned above, A_{21}, B_{12} and B_{21} are Einstein coefficients. Equations (1.13) are very important because they show a connection between the described radiation processes which are fundamental for describing laser operation.